

The Effect of Guest Inclusion on the Crystal Packing of *p*-*tert*-Butylcalix[4]arenes

Salvador León,^{*[a]} David A. Leigh,^{*[b]} and Francesco Zerbetto^{*[a]}

Abstract: The effect of guest inclusion in the crystal structures of *p*-*tert*-butylcalix[4]arene complexes has been investigated through a combination of molecular-mechanics-based solid-state calculations and statistical analysis, with a procedure previously developed and used to study a variety of classes of organic compounds. The results indicate that the general trends in the behavior of calixarene crystals are very similar, irrespective of the presence or the absence of a guest encapsulated in the calixarene

cavity, and are similar to those obtained for most other organics. Some differences arise only when a statistical analysis of several descriptors is performed. The investigation of the description of *endo* calix[4]arenes is extended by calculating the packing coefficient of the

Keywords: calixarenes • host–guest systems • macrocycles • molecular modeling • solid-state structures

guest inside the calixarenes cavity, C_k^{cavity} , which shows that most of them are well accommodated inside the host and have coefficients that are similar to those found in the liquid phase. Further evaluation of the interaction energies between guest and host shows that the coefficients tend to be smaller than 30 kcal mol⁻¹. The combination of small C_k^{cavity} and low interaction energies suggests that guest mobility in the solid could be rather common in *endo* complexes of calixarenes.

Introduction

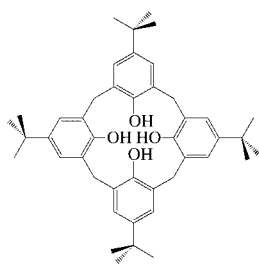
Increasing interest is being devoted to the design of artificial molecular devices.^[1] Mechanically interlocked compounds^[2, 3] and host–guest inclusion (*endo*) complexes^[4] have potential for new technological applications based on the exploitation of the presence of new degrees of freedom that originate from the motion that one component may undergo with respect to another. In the case of *endo* complexes formed by calixarenes and other bowl-shaped compounds, possible motions range from chemically induced changes in the orientation of the guest inside the cavity to exchange processes between binding sites. To date, the presence and effects of these motions are rather well established in solution for both mechanically interlocked compounds and *endo* complexes,^[5, 6] but only a small number of them have been seen in the solid phase,^[7, 8] where practical applications of such motions are likely to find first use.

In the crystalline state, guest motion can be “frozen” by intermolecular crystal packing interactions. In order for such dynamics to exist on a reasonably fast—that is, microsecond to second—timescale, the packing forces must be optimized. The forces bringing a molecular crystal together and the forces governing the guest motions are strongly connected, and their investigation can be carried out concomitantly. In a recent paper,^[9] we applied to crystals of benzylic amide macrocycle-containing (BAMC) rotaxanes the approach pioneered by Gavezzotti and co-workers for describing the structural properties of various classes of organic crystals. The model is based on a combination of crystal-structure analyses and molecular-mechanics calculations and has been quite successful.^[10] Our study provided clues about the description of BAMC rotaxanes in the solid and allowed the prediction of which of these systems were most likely to show condensed-phase dynamics triggered by an external stimulus. The predictions were confirmed by subsequent Atomic Force Microscopy experiments.

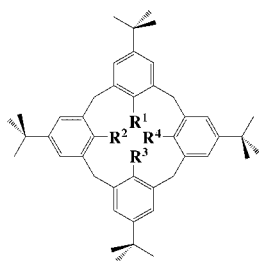
An interesting question connected to that work is whether the behavior and the properties of BAMC rotaxanes (and mechanically interlocked compounds in general) can be extrapolated to other inclusion complexes, and which similarities and differences can be expected. In this work, we extend the approach to the study of an important class of inclusion complexes formed by bowl-shaped host molecules with guests encapsulated in their cavities. They are one of the most studied families of calix[4]arenes, that is, the complexes of *p*-*tert*-butylcalix[4]arene derivatives with neutral organic

[a] Dr. S. León, Prof. F. Zerbetto
Dipartimento di Chimica “G. Ciamician”
Università degli Studi di Bologna
via F. Selmi 2, 40126 Bologna (Italy)
Fax: (+39)051-2099456
E-mail: gatto@ciam.unibo.it

[b] Prof. D. A. Leigh
School of Chemistry, University of Edinburgh
The King’s Buildings, West Mains Road
Edinburgh, EH9 3JJ (UK)
Fax: (+44) 131-667-9085
E-mail: david.leigh@ed.ac.uk

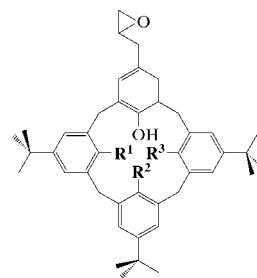


Ref.	Guest
1	QIGBEN self-inclusion
2a	LODNOH carbon disulfide
2b	LODNOH01 carbon disulfide
3	ZAHMOK acetonitrile
4	VEGPIG dimethyl sulfoxide
5	NILCAM pentane
6	NILCEQ 1-chlorobutane
7	NILCIU 1,3-dichloropropane, water
8	NILCOA 1-butanol
9	XAHMOI 1,4-butanediamine
10	QIGBAJ tetradecane
11	GOKPEB benzene
12	GOKQUS pyridine
13	BHPMYC01 toluene
14	BOCZUO fluorobenzene
15	CUPWAL anisole
16a	NAPCEM nitrobenzene
16b	NAPCIQ nitrobenzene (propane)
16c	RUFPIR nitrobenzene (xenon)

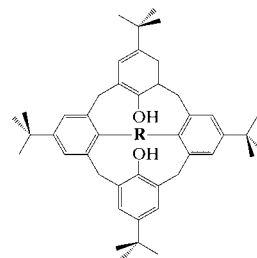


Ref.	Substituents	Guest
17	SIVMOZ $R^1 = R^2 = R^3 = R^4 = -H$	
18	SIVMEP $R^1 = -H$; $R^2 = R^3 = R^4 = -OH$	pyridine, benzene
19	SOQBII $R^1 = R^2 = -CH_3$; $R^3 = R^4 = -OH$	
20	SOQBOP $R^1 = R^2 = -CH_3$; $R^3 = R^4 = -OCH_3$	
21	KUGVUD $R^1 = R^2 = -OH$; $R^3 = R^4 = -OCH_2CH_3$	ethanol
22	GIYTEN $R^1 = R^2 = R^3 = R^4 = -OCH_2CH_2CH_3$	acetonitrile
23	SUVLEA $R^1 = R^3 = -OCH_2CH_2CH_3$; $R^2 = R^4 = -OCH_2CH_2OH$	
24	CIUROC $R^1 = R^3 = -OCH_2CH_2COOH$; $R^2 = R^4 = -OCH_2CH_2OCH_3$	methanol
25	WAZXOK $R^1 = R^2 = R^3 = R^4 = -OCH_2CH_2OCH_3$	
26	DUTBUP $R^1 = R^2 = R^3 = R^4 = -OCOOCH_2CH_3$	acetonitrile
27	GIYTOX $R^1 = R^2 = R^3 = R^4 = -OCH_2COOCH_2CH_3$	acetonitrile
28	VUHDEH $R^1 = R^2 = R^3 = R^4 = -OCH_2COOCH_2CF_3$	
29	NECVUM $R^1 = R^2 = R^3 = R^4 = -OCONHCH_2CH_2CH_2CH_3$	ethanol, water
30	JEGQOB $R^1 = -OCH_2CH_2N(CH_2CH_3)_2$	
31	WOJMEN $R^1 = R^3 = -OH$; $R^2 = R^4 = -OCH_2$	carbon tetrachloride, diiodotetrafluorobenzene
32	JORSEO $R^1 = R^3 = -OCH_2COOCH_2CH_3$; $R^2 = R^4 = -OCH_2$	acetonitrile
33a	JOYHAG $R^1 = R^2 = R^3 = R^4 = -OCH_2$	methanol

33b	JOYHIO $R^1 = R^2 = R^3 = R^4 = -OCH_2$	methanol
34	WOHBAW $R^1 = R^3 = -OCH_2CON(CH_2CH_3)_2$; $R^2 = R^4 = -OCH_2$	acetonitrile
35	JIQSIL $R^1 = R^3 = -OH$; $R^2 = R^4 = OCH_2$	
36	KOMTAH $R^1 = R^2 = -OH$; $R^3 = R^4 = -CO$	
37	MECWUM $R^1 = R^3 = -OH$; $R^2 = R^4 = -CO$	acetone
38	ZUDDIL $R^1 = R^2 = R^3 = R^4 = -OCH_2$	
39	HEKWID $R^1 = R^2 = R^3 = R^4 = -OCH_2COO$	
40	KEQYAG $R^1 = R^2 = R^3 = R^4 = -OCH_2CONH$	
41	KEGYEK $R^1 = R^2 = R^3 = R^4 = -OCH_2CONH$	furfuraldehyde, methanol, water
42	DOBBEB $R^1 = R^3 = -OH$; $R^2 = R^4 = -OCH_2CONHCH_2$	
43	DOBBIF $R^1 = R^3 = -OH$; $R^2 = R^4 = -OCH_2CH_2NHCO$	
44	ROKRAK $R^1 = R^3 = -OH$; $R^2 = R^4 = -OCH_2CH_2N=CH$	



Ref.	Substituents	Guest
45	CANQIR $R^1 = R^2 = R^3 = R^4 = CO$	hexane



Ref.	Substituents	Guest
46	CAZCUB $R = -OCH_2[CH_2OCH_2]_2CH_2O-$	chloroform
47	GILCAF $R = -OCH_2[CH_2OCH_2]_4CH_2O-$	pyridine
48	DOBBEF $R = -OCH_2CONH$ $NHCOCH_2O-$	dichloromethane, methanol
49	DOBHAD $R = -OCH_2CH_2NHCO$ $CONHCH_2CH_2O-$	acetonitrile

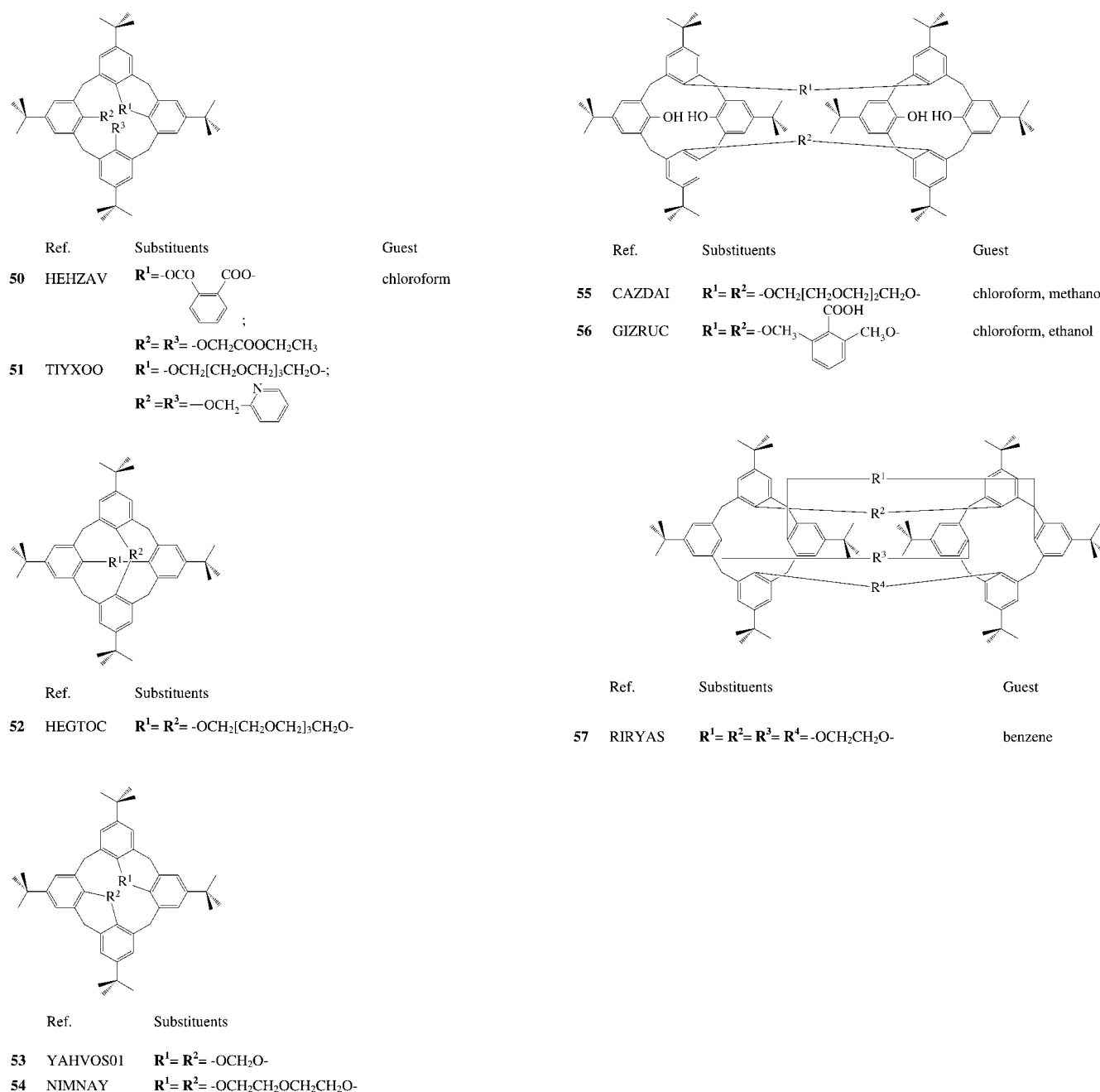


Figure 1. Pictorial representation of the *p*-*tert*-butylcalix[4]arene derivatives considered in this work.

molecules. Comparison of the results for calixarenes and other organics highlights differences and similarities between host–guest systems and more standard molecular crystals. The investigation is then extended to describe the packing coefficients of the guest inside the calixarene cavity, C_k^{cavity} . When compared with the standard packing coefficients in solution and with energies of interactions, C_k^{cavity} can be used as a possible indicator of mobility in the solid.

Selection of the structures: Structures of *p*-*tert*-butylcalix[4]arene derivatives, both corresponding to “molecule-within-molecule” or *endo* complexes and to “guest-free” structures or *exo* complexes, were retrieved from the Cambridge Structural Database (CSD).^[11]

From the data set, structures with metal atoms or ions and those deposited without coordinates were removed. In the case of disorder of the guest (when more than one set of coordinates is provided, or the coordinates are incomplete), one geometry was selected as the initial starting point (see next section). It must be mentioned that these structures usually have similar energies and similar crystal descriptors. The study of disorder remains a very interesting topic, but is outside the scope of this initial work.

The final set contained 61 structures, see Figure 1 (1–57), 19 of them corresponding to the unsubstituted ($R^1 \equiv R^2 \equiv R^3 \equiv R^4 \equiv \text{-OH}$) *p*-*tert*-butylcalix[4]arene (1–16a, b, c); 50 corresponding to calixarene molecules in a cone conformation (either with C_4 or C_2 symmetry), six were in partial cone

(paco) conformations, two in 1,2-alternate conformations, and three in 1,3-alternate conformations.

The structures of *p*-*tert*-butylcalix[4]arene derivatives with neutral guests or guest-free may be classified as: 1) guest-free structures and *exo* complexes, 2) 1:1 and 2:1 host–guest complexes,^[8b, 12] 3) hydrogen-bonded structures with amine

guests,^[13] 4) the recently observed self-inclusion structure, and 5) 1:1 host–guest clay-mimic structures.^[14] Table 1 summarizes both the conformations and the structural motifs of the systems considered in this work, while Figure 2 shows an example of each structural motif.

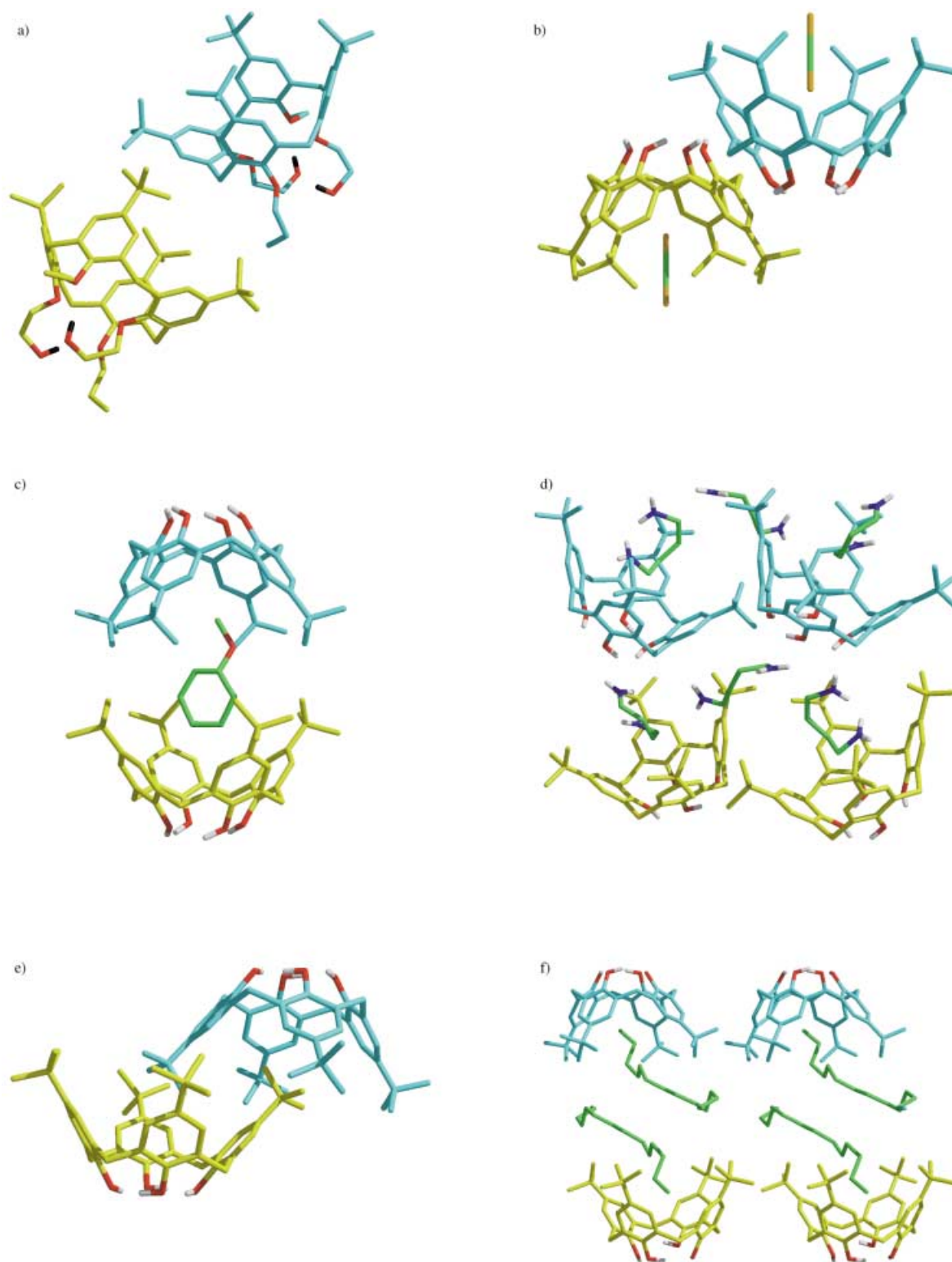


Figure 2. Examples of the structural motifs of *p*-*tert*-butylcalix[4]arene derivatives: a) guest-free structure **23**; b) 1:1 host–guest complex **2a**; c) 2:1 host–guest complex **15**; d) hydrogen-bonded structure **9** with an amine guest; e) self-inclusion structure **1**; and f) 1:1 host–guest clay-mimic structure **10**.

Table 1. Conformation, structural motifs, and energy contributions [kcal mol⁻¹] for the structures of *p*-*tert*-butylcalix[4]arene derivatives.

	RefCode	Conformation ^[a]	Motif ^[b]	PE	E _{Hbond}	E _π	E _{v_dW}
1	QIGBEN	cone	F	76.7	0.0	43.2	33.5
2a	LODNOH	cone	B	79.1	0.0	27.8	51.3
2b	LODNOH01	cone	B	80.7	0.0	26.2	54.5
3	ZAHMOK	cone	B	82.3	0.0	32.9	49.4
4	VEGPIG	cone	B	80.9	0.0	30.7	50.2
5	NILCAM	cone	B	82.1	0.0	34.1	48.0
6	NILCEQ	cone	B	85.4	0.0	33.9	51.6
7	NILCIU	cone	B	80.9	0.0	29.0	51.9
8	NILCOA	cone	B	84.4	0.0	31.6	52.8
9	XAHMOI	cone	D	69.3	1.6	29.9	37.7
10	QIGBAJ	cone	E	70.3	0.0	29.8	40.5
11	GOKPEB	cone	B	82.3	0.0	41.9	40.4
12	GOKQUS	cone	B	84.1	0.0	41.2	42.9
13	BHPMYC01	cone	B	81.5	0.0	42.4	39.1
14	BOCZUO	cone	B	82.0	0.0	39.7	42.3
15	CUPWAL	cone	C	77.8	0.0	37.1	40.7
16a	NAPCEM	cone	B	86.4	0.0	44.4	42.1
16b	NAPCIQ	cone	B	81.8	0.0	38.6	43.2
16c	RUFPIR	cone	B	86.5	0.0	44.4	42.1
17	SIVMOZ	1,3	A	74.9	0.0	43.1	31.8
18	SIVMEP	cone	B	79.2	0.0	51.8	27.4
19	SOQBIJ	1,3	A	69.5	0.0	34.8	34.7
20	SOQBOP	paco	A	69.1	0.0	32.5	36.6
21	KUGVUD	cone	B	79.5	0.0	33.9	45.6
22	GIYTEN	cone	B	93.2	0.0	33.1	60.0
23	SUVLEA	cone	A	74.0	0.0	30.1	44.0
24	CIJROC	cone	A	84.5	2.1	32.4	49.9
25	WAZXOK	cone	A	58.8	0.0	21.6	37.2
26	DUTBUP	cone	B	89.9	0.0	39.2	50.7
27	GIYTOX	cone	B	110.7	0.0	39.0	71.6
28	VUHDEH	cone	A	99.6	0.0	28.7	70.9
29	NECVUM	cone	A	80.1	1.8	24.4	54.0
30	JEGQOB	cone	A	92.4	0.0	28.9	63.6
31	WOJMEN	cone	A	90.1	0.0	39.2	51.0
32	JORSEO	paco	B	109.2	0.0	56.5	52.8
33a	JOYHAG	cone	A	106.2	2.1	68.5	35.6
33b	JOYHIO	paco	A	106.8	5.6	64.0	37.2
34	WOHBAW	cone	A	101.2	0.0	62.8	38.4
35	JIQSIL	cone	A	103.7	0.0	77.6	26.1
36	KOMTAH	paco	A	97.5	0.0	51.8	45.7
37	MECWUM	cone	B	123.2	7.1	59.6	56.5
38	ZUDDIL	cone	A	178.8	0.0	134.9	43.9
39	HEKWID	cone	A	116.1	0.0	76.0	40.1
40	KEQYAG	cone	A	130.0	3.4	82.2	44.4
41	KEQYEK	cone	F	116.2	5.8	65.6	44.8
42	DOBBEB	cone	F	100.5	0.0	63.6	36.9
43	DOBBIF	cone	A	80.9	0.0	18.6	62.3
44	ROKRAK	cone	A	89.8	0.0	50.0	39.8
45	CANQIR	paco	A	94.1	0.0	59.4	34.7
46	CAZCUB	cone	B	90.0	0.0	22.8	67.3
47	GILCAF	cone	B	77.2	0.0	34.8	42.4
48	DOBFEF	cone	B	104.4	1.4	36.5	66.5
49	DOBHAD	cone	B	100.1	0.0	46.8	53.4
50	HEHZAV	paco	B	101.6	1.5	50.7	49.5
51	TIYXOO	1,2	A	95.5	0.0	54.8	40.7
52	HEGTOC	1,3	A	60.1	0.0	19.8	40.4
53	YAHVOS01	cone	A	70.3	0.0	34.5	35.9
54	NIMNAY	1,2	A	71.5	0.0	31.3	40.2
55	CAZDAI	cone	B	152.1	1.6	39.9	110.6
56	GIZRUC	cone	B	172.4	6.1	53.7	112.6
57	RIRYAS	cone	A	85.5	0.0	52.7	32.8

[a] paco = partial cone, 1,2 = 1,2-alternate, 1,3 = 1,3-alternate. [b] A = guest-free and *exo* complexes, B and C = 1:1 and 2:1 host-guest *endo* complexes, respectively; D = hydrogen-bonded structures with amine guests; E = clay-mimic structures; F = self-inclusion structures.

Computational Methods

The molecular structures of the calixarenes were optimized subject to periodic boundary conditions and starting from the coordinates reported in the CSD. The periodic boundary conditions were applied with the minimum image convention, except for the cases where the size of the unit cell was too small compared to the cut-off distance of the interatomic potential (in this case, the program replicates the cell automatically). The minimization was necessary to avoid the effects of disorder that may be present for some systems. As mentioned before, the treatment of disorder, although interesting, is outside the scope of this initial work. The minimizations, with no symmetry constraints, were carried out with the MM3 force field^[15] implemented in the TINKER package.^[16] This model has been used in the past for calix[4]arenes^[8b, 17] (see also below).

For each of the minimized structures, the packing energy, PE , was calculated together with the molecular van der Waals surface, S_m , volume, V_m , and the Kitaigorodski packing coefficient, C_k , that is, the ratio of the occupied to the total volume of the unit cell. The atomic radii used to evaluate S_m , V_m , and C_k were taken from the work of Gavezzotti and co-workers on various organic systems,^[10] and were the same previously used for the study of crystal packing in BAMC rotaxanes.^[9]

Additionally, a recently proposed molecular descriptor, the packing coefficient of the host cavity (C_k^{cavity}),^[18] was calculated for structures that correspond to host–guest *endo* complexes. Its magnitude, defined as the volume ratio of the guest molecule to the host cavity, was estimated by calculating the volumes of the host cavities with the program Free Volume^[19] in the Cerius² software package (version 4.2).^[20] The calculation involves rolling of a spherical probe along the internal surface of the calixarene; a probe radius of 0.7 Å was used, in accordance to the work of Rebek and co-workers.^[18]

Solid-state validation of MM3 for calixarenes: In the past, models proposed by Allinger's group have been very successful in the description of calixarenes either in the isolated-molecule approximation or in solution.^[8b, 17] Several studies have shown that the MM3 force field can reproduce and predict the conformational properties and the energy profiles of calixarene isomer interconversions. Less attention has been devoted to the solid state. Recent *ab initio*^[21] work offers the opportunity to compare this approach with more computationally intensive data and to set the limits of accuracy one can expect for the calculations. Table 2 gives a comparison of the most relevant crystal parameters obtained experimentally, by *ab initio* methods, and by MM3 calculations for **2b** and **13**. The structural parameters obtained from MM3 minimizations compare well with both the experimental ones and those obtained from *ab initio* calculations; sometimes they are closer to the experimental ones than the *ab initio* data. A similar table containing the comparison of experimental and calculated structural parameters for the other systems can be obtained from one of the authors (S.L.).

Table 2. Comparison between experimental, *ab initio*,^[21] and MM3 structural parameters of crystal structures of **2b** and **13**. Angles are in degrees, distances in Å.

2b	Exp.	Ab initio	MM3	13	Exp.	Ab initio	MM3
Angles				Angles			
Ar-O ₄ ^[a]	123.5	124.6, 124.8 124.7, 125.1 124.5, 124.9 124.5, 124.4	120.5, 120.6 120.6, 120.6 120.7, 120.7 120.7, 120.7	Ar-O ₄	126.0 118.0	123, 121 127, 128 122, 123 126, 126	118, 118 125, 125 118, 118 125, 125
O ₄ -CS ₂ tilt	0.0	0.93, 1.24	0.0, 0.0	toluene tilt	0.0	1.1, 3.8	0.5, 0.6
				interplanar angle ^[b]	22.1	19.9, 24.8	18.5, 18.5
Distances				Distances			
C(CS ₂)-O ₄	5.34	5.75, 5.80	5.62, 5.62	CH ₃ (tol)-O ₄	3.65	3.64, 3.66	3.63, 3.63
C-S	1.55	1.58, 1.60	1.54, 1.54				

[a] Ar represents the substituted phenyl rings, O₄ is the plane defined by the four phenol oxygen atoms of the calixarene. [b] Angle between the plane of the toluene molecule and the *pseudo* mirror plane intersecting two of the methylene C atoms of the calixarene.

Results

Formation of inclusion complexes of calixarenes may modify the crystal properties and, *inter alia*, give systems endowed with “crystal plasticity” (i.e., the possibility of deformations produced by small forces) or the presence of mobility of the guest. The first property might enable surface patterning with an atomic force microscopy tip, while guest mobility could be exploited to create solid-state switches. Both these properties can appear if some or several of the noncovalent bonding interactions in the crystal are small. A low density of the solid can assist the phenomena. As a rule, mobility in the solid state is initiated by the presence or absence of shape complementarity. Within a class of similar molecules, however, other considerations—such as the size of the packing energies, the densities, or the value of some specific host–guest interactions—may become more relevant, since shape complementarity will be similar. While every calixarene is worthy of investigation in its own right, the issue we address here is whether some general trend(s) can emerge from the systematic investigation of a comprehensive set of calixarene solid state structures. Such trends could be exploited to provide information on the mechanical and dynamical properties of the crystals.

The investigation is divided in several steps:

- Total energies and their individual components are calculated for the crystal structures.
- Several correlations and fits between the energies themselves and the crystal properties are attempted (only the successful ones are reported).
- Comparison is made between the properties of calixarenes and those of other organics.
- Several descriptors of the calixarenes crystals are evaluated and used for a Principal Component Analysis, PCA, that allows to establish which quantities are intrinsically connected in the description of the crystals of these molecules (for instance, packing energies and densities).

Importantly, for the *endo* complexes, further parameters will be considered, the most important of which is probably the packing coefficient of the cavity, C_k^{cavity} .

General trends in the crystal packing of *p-tert*-butylcalix[4]-arenes

Energies: Table 1 shows a summary of the calculated energies for all structures. The packing energies, PE , range from 58.8 to 178.8 kcal mol⁻¹. This range is mainly independent of whether the structure is an *endo* complex. The energies have been divided in π interactions (both π stacking and CH \cdots π), hydrogen-bonding interactions, and remaining van der Waals interactions.

The π interactions and the van der Waals terms give the largest contribution to the packing energy, as is expected from the presence of four phenyl rings in calix[4]arenes that can interact with their environment. On the other hand, intermolecular hydrogen bonding is almost negligible; this reflects a clear preference of the calixarenes for intramolecular hydrogen bonding. Table 1 also shows that *endo* complexes do not differ substantially from *exo* complexes.

Fittings: Some general trends correlating the energy and its components can be estimated simply by fitting. A fair correlation, $r=0.72$, was found between *PE* and the π electron energies, E_{π} , which is calculated explicitly by MM3; no direct correlation was obtained either by fitting *PE* versus $E_{\text{H-bonding}}$ or *PE* with the rest of the van der Waals interactions. The correlation probably arises from the fact that most of the *p-tert-butylcalix[4]arene* derivatives have similar packing arrangements, which are characterized by π stacking and $\text{CH}\cdots\pi$ interactions.

Comparison with other organics: To gain a general understanding of the calixarene crystals, it is important to compare the values of several molecular descriptors with those of other organic compounds. Figure 3a shows the variation of the Kitaigorodski packing coefficient with the packing energy of *p-tert-butylcalix[4]arene* derivatives, along with the values reported for several organic compounds.^[9, 10] The results indicate that calix[4]arenes display high packing coefficients, in the range of those small organic compounds.^[22]

Figure 3b–e illustrates the variation of the packing energy of calix[4]arenes with different size-related quantities such as i) the van der Waals molecular surface, ii) volume, iii) the molecular weight, iv) the number of non-hydrogen atoms.

From the set of Figure 3, it is apparent that the behavior of *p-tert-butylcalix[4]arenes* is very similar to that of small organic compounds. Correlation can be sought and a certain amount is found between the packing energy of calixarenes and size parameters (see Table 3). The correlation coefficients observed for the subset of the *endo* complexes is larger than that for the empty systems (it increases from $r\approx 0.80$ to $r\approx 0.95$).

Table 3. Correlations between *PE* and molecular size descriptors ($PE = aX + b$).

Magnitude	Series	r	a	b
S_m	guest free	0.80	0.09	9.93
	<i>endo</i> complexes	0.93	0.10	16.43
	guest free + <i>endo</i>	0.82	0.09	20.71
V_m	guest free	0.77	0.07	16.68
	<i>endo</i> complexes	0.93	0.08	25.36
	guest free + <i>endo</i>	0.78	0.06	33.67
W_m	guest free	0.81	0.07	19.54
	<i>endo</i> complexes	0.95	0.09	22.79
	guest free + <i>endo</i>	0.81	0.07	31.62
N_{nonH}	guest free	0.83	1.00	19.06
	<i>endo</i> complexes	0.95	1.21	22.17
	guest free + <i>endo</i>	0.82	0.94	30.98

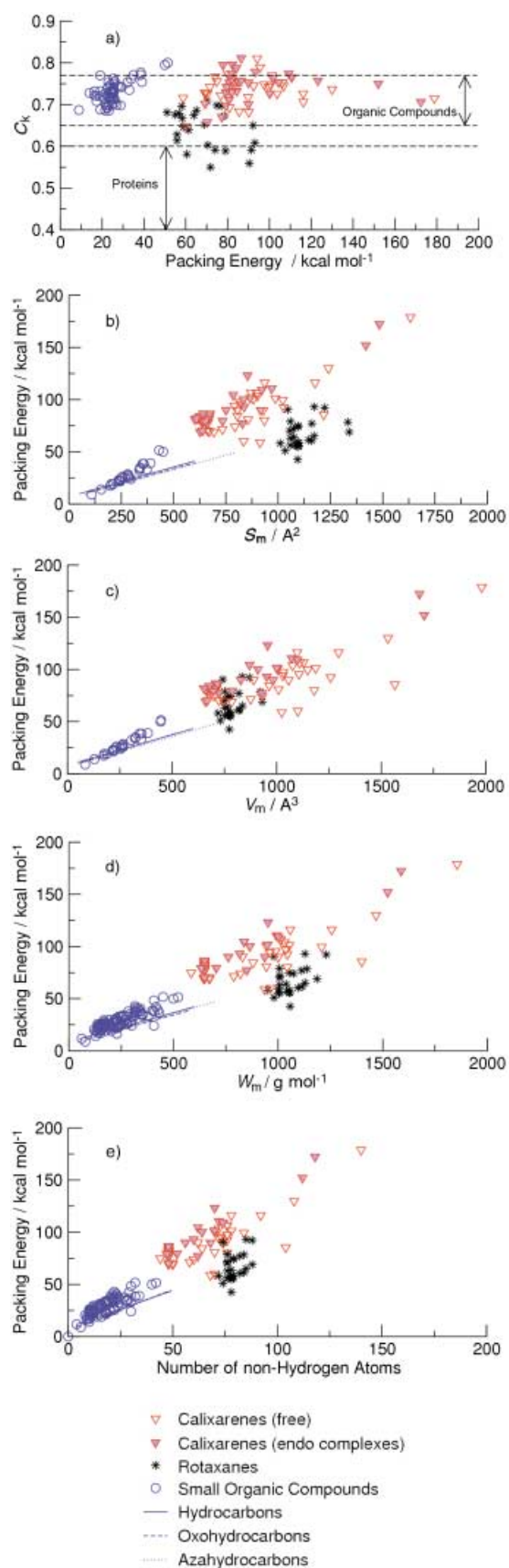


Figure 3. a) Variation of the Kitaigorodski packing coefficient, C_k , with the packing energy, *PE*; b) variation of *PE* with the molecular surface, S_m ; c) variation of *PE* with the molecular volume, V_m ; d) variation of *PE* with the molecular weight, W_m ; and e) variation of *PE* with the number of non-hydrogen atoms, N_{nonH} .

The origin of this effect is that the presence of a guest promotes the formation of the cone conformation, this, in turn, makes the subset more homogeneous and improves the correlation.

Apart from the improved fitting, comparison of the various kinds of descriptors for *endo* calix[4]arene complexes and the “empty” structure of the set of Figure 3 shows that the presence of a guest inside the host cage does not introduce significant changes in the packing properties of *p-tert*-butylcalix[4]arene derivatives.

Principal component analysis: In order to gain further insight, a principal component analysis (PCA) was performed, following previous work.^[9, 10] The scope is to follow in the steps of the systematic work performed by Gavezzotti and co-workers^[10] and to select, from the many possible descriptors of the crystal properties, the minimal amount that provides nearly all the information on the crystal properties.

The properties considered were the same as before^[9, 10] and are divided into:

- i) size parameters
 - a) the molecular weight, W_m
 - b) the number of valence electrons, Z_v
 - c) the molecular surface, S_m
 - d) the molecular volume, V_m
 - e) the packing energy, PE
 - f) the number of non-hydrogen atoms, N_{nonH}
- ii) stoichiometry parameters
 - g) the ratio of the number of non-hydrogen atoms over the number of hydrogen atoms, N_{nonH}/N_H
 - h) the ratio of the surface of the non-hydrogen atoms over the surface of the hydrogen atoms, S_{nonH}/S_H
 - i) the exposure ratio, V_m/S_m
- iii) packing parameters
 - j) the density, D_c
 - k) the number of electrons per unit volume in the cell, D_{el}
 - l) the Kitaigorodski packing coefficient, C_k
- iv) In addition, the π -energy contribution E_π to PE was included in the PCA.

The results of this PCA for *p-tert*-butylcalix[4]arene derivatives are summarized in Tables 4 and 5, which show the correlations matrix and the composition of the PCA matrix eigenvectors. In practice, of the 13 crystal descriptors, only five of their combinations are independent: the 13-dimen-

Table 5. Composition of the factors in the PCA for *p-tert*-butylcalix[4]arene derivatives. Coefficients < 0.1 in absolute values are omitted.

Eigenvalues	1	2	3	4	5
Value	6.97	2.64	1.27	0.82	0.64
% of variability	54	20	10	6	5
Cumulative %	54	74	84	90	95
Vectors	1	2	3	4	5
W_m	0.37	-0.10			0.10
Z_v	0.37	-0.12			0.12
S_m	0.36	-0.14		-0.19	
V_m	0.36	-0.15	-0.13		
PE	0.33			-0.37	-0.22
N_{nonH}	0.37	-0.10			
E_π	-0.27				0.76
N_{nonH}/N_H	0.24	0.32	0.40	0.23	0.11
V_m/S_m	0.22	-0.11	-0.25	0.76	0.18
S_{nonH}/S_H	0.15	0.29	0.60	0.23	
D_c	0.12	0.47		-0.30	0.43
D_{el}		0.57	-0.17		
C_k		0.40	-0.58	0.20	-0.29

sional space is reduced to 5-dimensional space with only 5% loss of information. The first three eigenvectors are very similar to those obtained in PCA for hydrocarbons^[10] and BAMC rotaxanes.^[9] The first eigenvector is mainly dominated by size parameters ($\approx 70\%$), and the second and the third correspond to in-phase and out-of-phase combinations of packing and stoichiometry parameters. The fourth eigenvector is mainly related to V_m/S_m , and the fifth to E_π . It is worth emphasizing that π interactions play a major role in the crystal structure of calixarenes, and one of the quantities associated with it, E_π , is independent in the PCA and cannot be described by a combination of the other descriptors. This emphasizes the role of π interactions in these systems.

General trends in the crystal packing of *endo* complexes of *p-tert*-butylcalix[4]arenes

Energy: The behavior of the structures corresponding to the subset of the *endo* host–guest complexes was also inspected separately. Table 6 shows the energy contributions to the interaction between the host and the guest, $E_{\text{H-G}}$, and between the guest and the external environment, $E_{\text{G-XI}}$. The $E_{\text{H-G}}$ interactions range from 7.1 to 20.1 kcal mol⁻¹, while the $E_{\text{G-XI}}$

Table 4. PCA correlations matrix for the structures of *p-tert*-butylcalix[4]arene derivatives.

	W_m	Z_v	S_m	V_m	PE	N_{nonH}	E_π	N_{nonH}/N_H	V_m/S_m	S_{nonH}/S_H	D_c	D_{el}	C_k
W_m	1.00	1.00	0.98	0.99	0.81	1.00	-0.62	0.51	0.60	0.30	0.21	0.00	-0.15
Z_v	1.00	1.00	0.98	0.99	0.80	1.00	-0.59	0.48	0.59	0.26	0.20	-0.02	-0.15
S_m	0.98	0.98	1.00	0.98	0.82	0.98	-0.59	0.39	0.49	0.20	0.18	-0.05	-0.17
V_m	0.99	0.99	0.98	1.00	0.78	0.99	-0.59	0.40	0.64	0.18	0.15	-0.07	-0.13
PE	0.81	0.80	0.82	0.78	1.00	0.82	-0.72	0.51	0.27	0.30	0.43	0.22	0.08
N_{nonH}	1.00	1.00	0.98	0.99	0.82	1.00	-0.64	0.51	0.60	0.29	0.20	-0.01	-0.15
E_π	-0.62	-0.59	-0.59	-0.59	-0.72	-0.64	1.00	-0.54	-0.34	-0.40	-0.19	-0.13	-0.08
N_{nonH}/N_H	0.51	0.48	0.39	0.40	0.51	0.51	-0.54	1.00	0.32	0.77	0.53	0.46	0.01
V_m/S_m	0.60	0.59	0.49	0.64	0.27	0.60	-0.34	0.32	1.00	0.07	0.00	-0.07	0.10
S_{nonH}/S_H	0.30	0.26	0.20	0.18	0.30	0.29	-0.40	0.77	0.07	1.00	0.31	0.37	-0.06
D_c	0.21	0.20	0.18	0.15	0.43	0.20	-0.19	0.53	0.00	0.31	1.00	0.72	0.38
D_{el}	0.00	-0.02	-0.05	-0.07	0.22	-0.01	-0.13	0.46	-0.07	0.37	0.72	1.00	0.70
C_k	-0.15	-0.15	-0.17	-0.13	0.08	-0.15	-0.08	0.01	0.10	-0.06	0.38	0.70	1.00

Table 6. Energy contributions [kcal mol⁻¹] to guest–host and guest–environment interactions for the *endo* complexes of *p*-*tert*-butylcalix[4]arene derivatives.

RefCode	Guest	E_{H-G}				E_{G-Xt}				
		E_{Total}	E_{Hbond}	E_{π}	E_{vdW}	E_{Total}	E_{Hbond}	E_{π}	E_{vdW}	
2a	LODNOH	carbon disulfide	8.9	0.0	0.0	8.9	3.5	0.0	0.0	3.5
2b	LODNOH01	carbon disulfide	8.8	0.0	0.0	8.8	3.8	0.0	0.0	3.8
3	ZAHMOK	acetonitrile	10.9	0.0	2.7	8.2	3.4	0.0	0.1	3.3
4	VEGPIG	DMSO	12.4	0.0	2.4	10.0	2.3	0.0	0.1	2.2
5	NILCAM	pentane	9.6	0.0	5.2	4.4	6.5	0.0	1.1	5.4
6	NILCEQ	chlorobutane	9.4	0.0	5.1	4.4	8.3	0.0	0.4	7.9
7	NILCIU	dichloropropane	10.9	0.0	2.1	8.8	7.8	0.0	0.1	7.7
8	NILCOA	butanol	13.6	0.0	5.8	7.8	5.3	0.0	0.6	4.8
9	XAHMOI	butanediamine	12.9	0.0	6.5	6.4	14.8	4.4	2.1	8.4
10	QIGBAJ	tetradecane	9.8	0.0	5.6	4.3	13.0	0.0	0.8	12.2
11	GOKPEB	benzene	10.7	0.0	7.3	3.4	4.4	0.0	2.0	2.4
12	GOKQUS	pyridine	11.0	0.0	7.1	3.9	4.7	0.0	2.0	2.7
13	BHPMYC01	toluene	12.3	0.0	7.0	5.3	5.9	0.0	2.4	3.5
14	BOCZUO	fluorobenzene	10.9	0.0	6.7	4.2	5.1	0.0	1.5	3.6
15	CUPWAL	anisole	20.1	0.0	11.6	8.5	1.4	0.0	0.4	1.0
16a	NAPCEM	nitrobenzene	14.0	0.0	7.3	6.7	8.1	0.0	2.0	6.1
16b	NAPCIQ	nitrobenzene	11.8	0.0	6.5	5.3	8.4	0.0	1.4	7.1
16c	RUFPIR	nitrobenzene	14.0	0.0	7.2	6.7	8.1	0.0	1.9	6.1
18	SIVMEP	pyridine	12.1	0.0	8.0	4.1	5.9	0.0	2.9	3.0
21	KUGVUD	ethanol	7.2	0.0	4.2	2.9	4.5	0.0	0.3	4.2
22	GIYTEN	acetonitrile	12.3	0.0	2.2	10.1	2.6	0.0	0.0	2.6
26	DUTBUP	acetonitrile	10.5	0.0	2.0	8.5	2.6	0.0	0.0	2.6
27	GIYTOX	acetonitrile	12.0	0.0	2.4	9.6	3.6	0.0	0.0	3.6
32	JORSEO	acetonitrile	10.2	0.0	1.1	9.1	2.4	0.0	0.1	2.3
37	MECWUM	acetone	11.2	0.0	2.0	9.2	3.5	0.0	0.0	3.5
46	CAZCUB	chloroform	11.8	0.0	1.2	10.5	4.8	0.0	0.0	4.8
47	GILCAF	pyridine	13.1	0.0	8.2	4.9	3.6	0.0	1.0	2.6
48	DOBFEF	dichloromethane	11.5	0.0	0.8	10.7	2.5	0.0	0.0	2.5
49	DOBHAD	acetonitrile	10.9	0.0	2.2	8.7	4.5	0.0	0.2	4.3
50	HEHZAV	methanol	10.1	1.5	4.5	4.1	1.4	0.0	0.1	1.3
55	CAZDAI	methanol	11.5	0.0	6.6	4.9	2.9	0.0	0.0	2.9
56	GIZRUC	ethanol	12.3	0.0	6.6	5.7	0.8	0.0	0.0	0.8

range from 0.8 to 14.8 kcal mol⁻¹. In general, the intracomplex interactions are larger than the interaction between the guest and the environment (see also below). This feature is caused by the full embedding of the guest molecule inside the calixarene cavity. Only for compounds **9** and **10** is the intercomplex energy higher than the intracomplex energy. In **9**, the guest (butanediamine) forms a network of intermolecular hydrogen bonds in the crystal; in **10**, the guest molecule (tetradecane) is so large that part of it is not encapsulated inside the host cage.

Of the various energy terms, the π interactions and the van der Waals interactions provide, as before, the largest contributions. This is in agreement with the important role generally attributed to π stacking and CH \cdots π energies in *endo* complexes of calixarenes.^[8c, 23]

Fittings: A very good correlation, $r = 0.98$, is found between the *PE* of the *endo* complex and the intermolecular energy of the host calix[4]arene molecule. Similar good correlations are found if one considers *PE*, the energy of interaction of the host with its environment, versus the three energy components (hydrogen bond energy, π energies, and other van der Waals energy). In practice, the *PE* of the *endo* complexes of calix[4]arenes is mainly due to the intermolecular energy of the host calixarene.

Principal component analysis: A second PCA, which included some additional parameters, was performed just for the *endo* complexes of *p*-*tert*-butylcalix[4]arene. The new parameters were:

- E_{H-G} , the interaction energy of the host calixarene with the guest,
- E_{G-Xt} , the interaction energy of the guest with the rest of its environment,
- $E_{\pi(\text{inter})}$, the intercomplex π energy of the complex;
- $E_{\pi(\text{intra})}$, the π energy for the interaction between the host and the guest,
- $E_{\pi(\text{guest})}$, the intercomplex π energy of the guest,
- C_k^{cavity} , the packing coefficient of the host cavity (this term is described more in detail below).

The results of the PCA on the descriptors of the crystals of the *endo* complexes are shown in Tables 7 and 8. Of the 18 crystal descriptors only seven of their combinations suffice to describe the crystal properties: the 18-dimensional space is reduced to 7-dimensional space with 6% loss of information. The first eigenvector is very similar to the first one of the former PCA, being mainly related to size parameters. The other six eigenvectors basically correspond to a complex mixing of the other parameters; in particular, energy parameters are rather important components in all these eigenvectors.

Table 7. PCA correlations matrix for the *endo* complexes of *p*-*tert*-butylcalix[4]arene derivatives.

	<i>PE</i>	<i>E</i> _{H-G}	<i>E</i> _{G-Xt}	<i>E</i> _{π(inter)}	<i>E</i> _{π(intra)}	<i>E</i> _{π(guest)}	<i>W</i> _m	<i>Z</i> _v	<i>S</i> _m	<i>V</i> _m	<i>N</i> _{nonH}	<i>N</i> _{nonH} / <i>N</i> _H	<i>V</i> _m / <i>S</i> _m	<i>S</i> _{nonH} / <i>S</i> _H	<i>D</i> _c	<i>D</i> _{el}	<i>C</i> _k	<i>C</i> _k ^{cavity}
<i>PE</i>	1.00	-0.12	-0.36	0.29	-0.13	-0.37	0.93	0.92	0.66	0.67	0.93	-0.15	0.35	0.25	0.57	0.18	0.01	-0.48
<i>E</i> _{H-G}	-0.12	1.00	-0.06	-0.19	0.58	0.21	0.02	0.02	0.35	0.36	0.03	0.15	0.18	-0.07	0.00	0.07	0.28	0.26
<i>E</i> _{G-Xt}	-0.36	-0.06	1.00	-0.29	0.23	0.52	-0.39	-0.37	-0.35	-0.42	-0.39	0.05	-0.41	-0.18	-0.29	-0.08	-0.23	0.69
<i>E</i> _{π(inter)}	0.29	-0.19	-0.29	1.00	-0.18	0.10	0.14	0.12	-0.09	-0.01	0.16	-0.17	0.31	0.37	0.28	0.47	0.24	-0.29
<i>E</i> _{π(intra)}	-0.13	0.58	0.23	-0.18	1.00	0.65	-0.02	0.03	0.28	0.29	0.03	-0.18	0.18	-0.43	-0.17	-0.05	0.14	0.48
<i>E</i> _{π(guest)}	-0.37	0.21	0.52	0.10	0.65	1.00	-0.40	-0.38	-0.36	-0.32	-0.36	0.03	0.00	-0.30	-0.20	0.06	0.11	0.62
<i>W</i> _m	0.93	0.02	-0.39	0.14	-0.02	-0.40	1.00	1.00	0.82	0.83	1.00	-0.11	0.41	0.11	0.45	0.00	-0.12	-0.46
<i>Z</i> _v	0.92	0.02	-0.37	0.12	0.03	-0.38	1.00	1.00	0.83	0.84	1.00	-0.15	0.40	0.08	0.41	-0.02	-0.13	-0.45
<i>S</i> _m	0.66	0.35	-0.35	-0.09	0.28	-0.36	0.82	0.83	1.00	0.97	0.83	-0.24	0.34	-0.10	0.17	-0.18	-0.07	-0.36
<i>V</i> _m	0.67	0.36	-0.42	-0.01	0.29	-0.32	0.83	0.84	0.97	1.00	0.83	-0.16	0.54	-0.13	0.27	-0.08	0.03	-0.36
<i>N</i> _{nonH}	0.93	0.03	-0.39	0.16	0.03	-0.36	1.00	1.00	0.83	0.83	1.00	-0.15	0.41	0.10	0.43	0.01	-0.11	-0.45
<i>N</i> _{nonH} / <i>N</i> _H	-0.15	0.15	0.05	-0.17	-0.18	0.03	-0.11	-0.15	-0.24	-0.16	-0.15	1.00	0.25	0.09	0.44	0.24	0.09	0.26
<i>V</i> _m / <i>S</i> _m	0.35	0.18	-0.41	0.31	0.18	0.00	0.41	0.40	0.34	0.54	0.41	0.25	1.00	-0.14	0.48	0.33	0.37	-0.11
<i>S</i> _{nonH} / <i>S</i> _H	0.25	-0.07	-0.18	0.37	-0.43	-0.30	0.11	0.08	-0.10	-0.13	0.10	0.09	-0.14	1.00	0.31	0.38	0.05	-0.26
<i>D</i> _c	0.57	0.00	-0.29	0.28	-0.17	-0.20	0.45	0.41	0.17	0.27	0.43	0.44	0.48	0.31	1.00	0.75	0.50	-0.09
<i>D</i> _{el}	0.18	0.07	-0.08	0.47	-0.05	0.06	0.00	-0.02	-0.18	-0.08	0.01	0.24	0.33	0.38	0.75	1.00	0.78	0.12
<i>C</i> _k	0.01	0.28	-0.23	0.24	0.14	0.11	-0.12	-0.13	-0.07	0.03	-0.11	0.09	0.37	0.05	0.50	0.78	1.00	0.03
<i>C</i> _k ^{cavity}	-0.48	0.26	0.69	-0.29	0.48	0.62	-0.46	-0.45	-0.36	-0.36	-0.45	0.26	-0.11	-0.26	-0.09	0.12	0.03	1.00

Table 8. Composition of the factors in the PCA for the *endo* complexes of *p*-*tert*-butylcalix[4]arene derivatives. Coefficients < 0.1 in absolute values have been omitted.

Eigenvalues	1	2	3	4	5	6	7
Value	6.59	3.08	2.82	1.38	1.32	0.97	0.73
% of variability	37	17	16	8	7	5	4
Cumulative %	37	54	69	77	84	90	94
Vectors	1	2	3	4	5	6	7
<i>PE</i>	0.35				0.29		0.10
<i>E</i> _{H-G}		-0.11	0.40		-0.35	0.47	-0.29
<i>E</i> _{G-Xt}	-0.23	-0.14	0.10		0.53	0.12	0.18
<i>E</i> _{π(inter)}		0.32		-0.51	0.21	-0.13	-0.42
<i>E</i> _{π(intra)}		-0.26	0.48	-0.21			
<i>E</i> _{π(guest)}	-0.20		0.35	-0.23	0.34	-0.13	-0.25
<i>W</i> _m	0.37				0.18		
<i>Z</i> _v	0.37	-0.11			0.19		
<i>S</i> _m	0.32	-0.25	0.11			0.16	
<i>V</i> _m	0.34	-0.19	0.17		-0.13		
<i>N</i> _{nonH}	0.37				0.19		
<i>N</i> _{nonH} / <i>N</i> _H		0.22	0.13	0.67		-0.17	-0.37
<i>V</i> _m / <i>S</i> _m	0.20	0.14	0.29		-0.14	-0.51	-0.24
<i>S</i> _{nonH} / <i>S</i> _H		0.31	-0.20		0.12	0.61	-0.38
<i>D</i> _c	0.20	0.39	0.16	0.27	0.13		0.17
<i>D</i> _{el}		0.48	0.23		0.10	0.15	0.24
<i>C</i> _k		0.36	0.31	-0.19	-0.26		0.45
<i>C</i> _k ^{cavity}	-0.23		0.33	0.22	0.30		

The conclusion is that formation of endohedral complexes does affect the crystal description, but in a way that is recognized only by a statistical analysis, and that π interactions, stoichiometry, and packing become intrinsically entangled upon inclusion.

The packing coefficient of the host cavity, C_k^{cavity} , deserves special attention: This descriptor is defined as the ratio of the guest volume to the host-cavity volume, and was recently introduced by Mecozzi and Rebek.^[18] In their study, they showed that the volumes of the guest and the host play an important role in molecular encapsulation. They found that the inclusion of the guest is most favorable when C_k^{cavity} approaches a value of 0.55, which corresponds to the packing

coefficient in the liquid phase. Figure 4 shows the variation of C_k^{cavity} with the molecular volume of the guest, V_m^{guest} , for the set of *endo p*-*tert*-butylcalix[4]arene complexes. Values calculated for the *endo* complexes of calixarene range from 0.29 to 0.64. This is similar to what was reported in the literature^[24] for several inclusion compounds (including also calix[4]arenes),^[24f,g] both in solution and in the solid state. C_k^{cavity} increases with the size of the guest, and a fair correlation between the two, $r = 0.75$, is found. The simple interpretation is that the guest molecules encapsulated in cavities modify the calixarenes' conformations. As stated before, structure **10** differs from the other complexes because the large tetradecane guest cannot be completely encapsulated

in the calixarene cage, and a considerable portion of it is found outside of the cavity. When this structure is excluded, the correlation between C_k^{cavity} and V_m^{guest} increases from $r = 0.75$ to $r = 0.83$.

Discussion and Conclusion

The description of the crystal properties of “empty” and *endo* complexes of *p*-*tert*-butylcalix[4]arene derivatives has been developed and discussed in terms of a combination of molecular modeling and statistical analysis, in analogy with what has previously been done for various classes of organic molecules. Total energies and their components, correlation

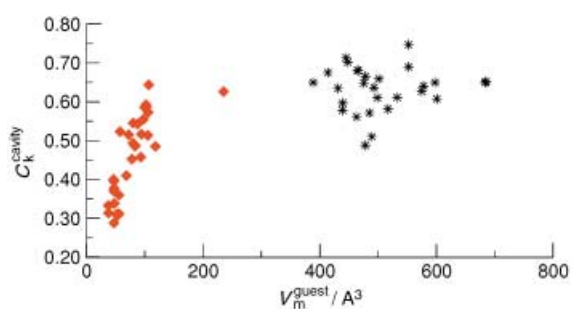


Figure 4. Variation of the packing coefficient of the host cavity, C_k^{cavity} , with the molecular volume of the guest, V_m^{guest} for the *endo p-tert-butylcalix[4]arene* complexes (red diamonds). Values for BAMC rotaxanes (black stars) are also displayed for comparison.

between different crystal descriptors, and the results of two principal component analyses have been presented and compared with similar data for other molecules. Of the two fundamental structural motifs present in calixarenes crystals, π interactions and H bonding, the first emerges as prominent, while the second hardly enters the description of the crystal properties.

One of the questions that arise is whether the calculations can provide information on guest mobility in the calix[4]arene cavities. There are several reports of this property for different complexes^[8] for unsubstituted *p-tert-butylcalix[4]arene* with acetone, chloroform, *p-xylene*, benzene, pyridine, and nitrobenzene. Only the structures of the three last systems (**11**, **12**, and **16a–c**) were available in the CSD. Acetone, chloroform, and pyridine *endo* complexes are also present in the CSD, but with different substituted *p-tert-butylcalix[4]arenes* (structures **18**, **37**, **46**, and **47**). Guest mobility requires a) weak interactions between the guest and its surrounding molecules and b) low C_k^{cavity} ; this implies a large amount of space available for the guest to move. Figure 5a shows a 3D plot of C_k^{cavity} , the host–guest interaction energy, the interaction energy of the guest and the crystal environment, Figure 5b displays the variation of C_k^{cavity} versus the sum of both energy components. It can be seen that many complexes present low values for the three quantities (C_k^{cavity} , $E_{\text{H-G}}$, and $E_{\text{G-Xt}}$), and that the sum of the total energy of interaction of the guest and host is always lower than 30 kcal mol⁻¹. In particular, the triangles embedded in circles in Figure 5b correspond to systems for which guest mobility in a crystal has been observed. Since they do not show any remarkable difference from the others for which mobility has not yet been observed, the calculations suggest that guest mobility in the crystal can be a general property of *endo* complexes of calix[4]arenes.

A second question that arises, also in view of previous work^[9] is how a different arrangement of some of the structural motifs of calixarenes can influence the outcome of the analysis. The structural motifs shared by calixarenes and the previously investigated BAMC rotaxanes are: a) H bonding, b) π stacking, c) presence of a macrocyclic ring, and d) presence of a guest inside this macrocyclic ring. Notice that in most *endo*-complexed calixarenes the host is entirely encapsulated inside the cavity, while in BAMC rotaxanes a rather large portion of the guest is outside and is in contact with other molecules.

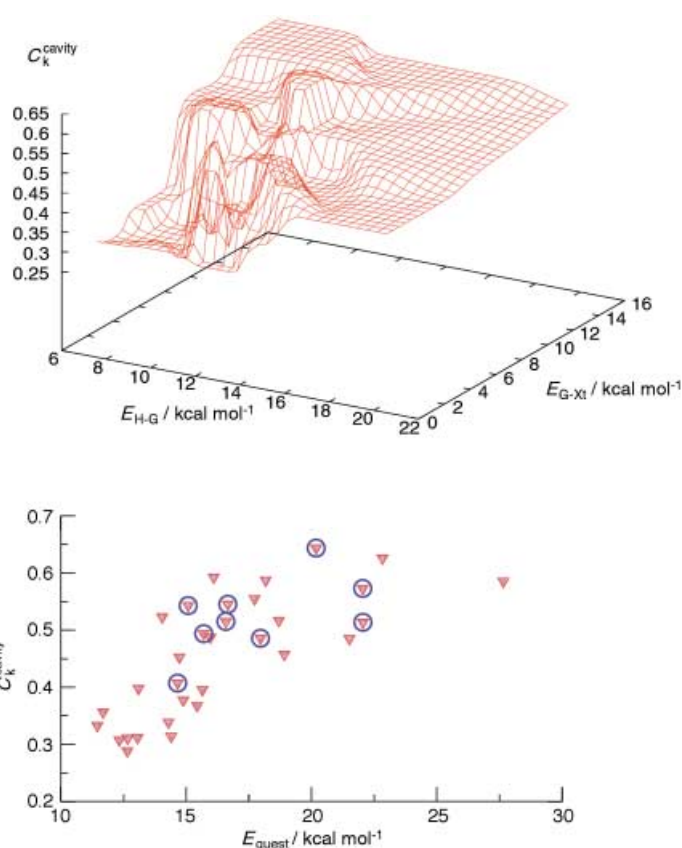


Figure 5. a) 3D plot of C_k^{cavity} versus the interaction energy the host–guest, $E_{\text{H-G}}$, and versus the interaction energy of the guest-crystal environment, $E_{\text{G-Xt}}$; b) variation of C_k^{cavity} with the sum of both energy components. Points corresponding to structures with a guest for which mobility within a crystal has been observed (**11**, **12**, **16a–c**, **18**, **37**, **46**, and **47**) are circled.

The comparison is best carried out in points:

- i) The Kitaigorodski packing coefficients of calix[4]arenes are markedly higher than those of BAMC rotaxanes, which are intermediate between those of organic crystals and protein.^[22]
- ii) Packing energies of calixarenes tend to be comparatively higher than those of BAMC rotaxanes.
- iii) Packing energies of calixarenes and size parameters tend to correlate, as is observed in organic compounds, while this does not occur for BAMC rotaxanes.
- iv) The correlation between packing energies and π -electron energies observed in calixarenes is not observed in BAMC rotaxanes, in which the dominant role is played by H bonds rather than π interactions.
- v) In the *endo* complexes of calixarenes, the *PE* is mainly due to the interaction of the calixarene with its environment. This is true to a much smaller extent for BAMC rotaxanes and reflects the difference in magnitude of the interaction between the guest and the environment for the two sets of compounds.
- vi) A correlation exists in *endo*-complexed calixarenes between the packing coefficient of the cavity, C_k^{cavity} , and the size of the guest—a similar correlation does not exist for the rotaxanes.
- vii) C_k^{cavity} for calixarenes are in the range 0.29–0.64, while for rotaxanes they are in the interval 0.51–0.74 (the liquid-

phase value of 0.55 is therefore best achieved by calixarenes).

- viii) The macrocycle–guest interaction energy is rather similar for calixarenes and for those BAMC rotaxanes for which solid-state mobility was proposed,^[9] and is below 30 kcal mol⁻¹.

The approach presented in this paper is based on a static picture of the crystals. The effect of disorder, although important, has been neglected both as a first approximation and because the crystal descriptors considered here are usually not influenced by it. Future work will have to include disorder and dynamics explicitly.

Acknowledgement

This work was supported by the TMR initiative of the European Union through contract HPRN-CT-2000-00024 (MIPA), the EPSRC and the MURST project “Dispositivi Supramolecolari”. D.A.L. is an EPSRC Advanced Research Fellow (AF/982324).

- [1] For recent reviews on artificial molecular machines, see “*Molecular Machines*” special issue, *Acc. Chem. Res.* **2001**, *34*, 409–522.
- [2] D. B. Amabilino, J. F. Stoddart, *Chem. Rev.* **1995**, *95*, 2725–2828.
- [3] *Molecular Catenanes, Rotaxanes, and Knots* (Eds.: J.-P. Sauvage, C. Dietrich-Buchecker), Wiley-VCH, Weinheim, **1999**.
- [4] For reviews on calixarenes, see: a) *Calixarenes, a Versatile Class of Macrocyclic Compounds* (Eds.: J. Vicens, V. Böhmer), Kluwer Academic, Dordrecht, **1991**; b) V. Böhmer, *Angew. Chem.* **1995**, *107*, 785–818; *Angew. Chem. Int. Ed. Engl.* **1995**, *34*, 713–745; c) A. Ikeda, S. Shinkai, *Chem. Rev.* **1997**, *97*, 1713–1734; d) C. D. Gutsche in *Monographs in Supramolecular Chemistry, Vol. 6: Calixarenes Revisited* (Ed.: J. F. Stoddart), The Royal Society of Chemistry, Cambridge, **1998**.
- [5] See, for example: a) P.-L. Anelli, N. Spencer, J. F. Stoddart, *J. Am. Chem. Soc.* **1991**, *113*, 5131–5133; b) R. A. Bissell, E. Córdoba, A. E. Kaifer, J. F. Stoddart, *Nature* **1994**, *369*, 133–137; c) A. C. Benniston, A. Harriman, V. M. Lynch, *J. Am. Chem. Soc.* **1995**, *117*, 5275–5291; d) J.-P. Collin, P. Gavina, J.-P. Sauvage, *Chem. Commun.* **1996**, 2005–2006; e) P.-L. Anelli, M. Asakawa, P. R. Ashton, R. A. Bissell, G. Clavier, R. Górski, A. E. Kaifer, S. J. Langford, G. Matternsteig, S. Menzer, D. Philp, A. M. Z. Slawin, N. Spencer, J. F. Stoddart, M. S. Tolley, D. J. Williams, *Chem. Eur. J.* **1997**, *3*, 1113–1135; f) A. S. Lane, D. A. Leigh, A. Murphy, *J. Am. Chem. Soc.* **1997**, *119*, 11092–11093; g) H. Murakami, A. Kawabuchi, K. Kotoo, M. Kunitake, N. Nakashima, *J. Am. Chem. Soc.* **1997**, *119*, 7605–7606; h) C. Gong, T. E. Glass, H. W. Gibson, *Macromolecules* **1998**, *31*, 308–313; i) A. M. Brouwer, C. Frochot, F. G. Gatti, D. A. Leigh, L. Mottier, F. Paolucci, S. Roffia, G. W. H. Wurpel, *Science* **2001**, *291*, 2124–2128.
- [6] See, for example: a) S. Shinkai, K. Araki, T. Matsuda, N. Nishiyama, H. Ikeda, I. Takasu, M. Iwamoto, *J. Am. Chem. Soc.* **1990**, *112*, 9053–9058; b) P. Timmerman, W. Verboom, F. C. J. M. van Veggel, W. P. van Hoorn, D. N. Reinhoudt, *Angew. Chem.* **1994**, *106*, 1313–1315; *Angew. Chem. Int. Ed. Engl.* **1994**, *33*, 1292–1295; c) P. Timmerman, W. Verboom, F. C. J. M. van Veggel, J. P. M. van Duynhoven, D. N. Reinhoudt, *Angew. Chem.* **1994**, *106*, 2437–2440; *Angew. Chem. Int. Ed. Engl.* **1994**, *33*, 2345–2348; d) A. M. A. van Wageningen, J. P. M. van Duynhoven, W. Verboom, D. N. Reinhoudt, *J. Chem. Soc. Chem. Commun.* **1995**, 1941–1942; e) F. Ohseto, T. Sakaki, K. Araki, S. Shinkai, *Tetrahedron Lett.* **1993**, *32*, 2149–2152; f) F. Ohseto, S. Shinkai, *Chem. Lett.* **1993**, 2045–2048; g) F. Ohseto, S. Shinkai, *J. Chem. Soc. Perkin Trans. 2* **1995**, 1103–1109; h) A. Ikeda, T. Tsudera, S. Shinkai, *J. Org. Chem.* **1997**, *62*, 3568–3574.
- [7] a) M. Cavallini, R. Lazzaroni, R. Zamboni, F. Biscarini, D. Timpel, F. Zerbetto, G. J. Clarkson, D. A. Leigh, *J. Phys. Chem. B* **2001**, *105*, 10826–10830; b) T. Gase, D. Grando, P.-A. Chollet, F. Kajzar, A. Murphy, D. A. Leigh, *Adv. Mater.* **1999**, *11*, 1303–1306; c) C. P. Collier, G. Matternsteig, E. W. Wong, K. Beverly, J. Sampaio, F. M. Raymo, J. F. Stoddart, J. R. Heath, *Science* **2000**, *289*, 1172–1175.
- [8] a) E. B. Brouwer, G. D. Enright, J. A. Ripmeester, *J. Am. Chem. Soc.* **1997**, *119*, 5404–5412; b) B. Paci, M. S. Deleuze, R. Caciuffo, J. Tomkinson, F. Uguzzoli, F. Zerbetto, *J. Phys. Chem. A* **1998**, *102*, 6910–6915; c) E. B. Brouwer, G. D. Enright, C. I. Ratcliffe, G. A. Facey, J. A. Ripmeester, *J. Phys. Chem. B* **1999**, *103*, 10604–10616; d) F. Benevelli, A. Bond, M. Duer, J. Klinowski, *Phys. Chem. Chem. Phys.* **2000**, *2*, 3977–3981; e) F. Benevelli, W. Kolodziejcki, K. Wozniak, J. Klinowski, *Phys. Chem. Chem. Phys.* **2001**, *3*, 1762–1768; f) E. B. Brouwer, G. D. Enright, C. I. Ratcliffe, J. A. Ripmeester, *Supramol. Chem.* **1996**, *7*, 79–83; g) E. B. Brouwer, G. D. Enright, J. A. Ripmeester, *Supramol. Chem.* **1996**, *7*, 143–145; h) K. A. Udachin, G. D. Enright, E. B. Brouwer, J. A. Ripmeester, *J. Supramol. Chem.* **2001**, *1*, 97–100.
- [9] F. Biscarini, M. Cavallini, D. A. Leigh, S. León, S. J. Teat, J. K. Y. Wong, F. Zerbetto, *J. Am. Chem. Soc.* **2002**, *124*, 225–233.
- [10] a) A. Gavezzotti, G. R. Desiraju, *Acta Crystallogr.* **1988**, *B44*, 427–434; b) A. Gavezzotti, *J. Chem. Soc. Perkin Trans. 2* **1995**, 1399–1404; c) D. C. Sorescu, B. M. Rice, D. L. Thompson, *J. Phys. Chem. A* **1999**, *103*, 989–998; d) A. Gavezzotti, *J. Am. Chem. Soc.* **1989**, *111*, 1835–1843; e) A. Gavezzotti, *J. Phys. Chem.* **1991**, *95*, 8948–8955; f) A. Gavezzotti, G. Filippini, *Acta Crystallogr.* **1992**, *B48*, 537–545; g) J. D. Dunitz, A. Gavezzotti, *Acc. Chem. Res.* **1999**, *32*, 677–684.
- [11] Cambridge Structural Database System, version 5.11; Cambridge Crystallographic Data Centre, 12 Union Road, Cambridge, CB2 1EZ, (UK).
- [12] E. B. Brouwer, J. A. Ripmeester, G. D. Enright, *J. Inclusion Phenom. Mol. Recognit. Chem.* **1996**, *24*, 1–17.
- [13] E. B. Brouwer, K. A. Udachin, G. D. Enright, C. I. Ratcliffe, J. A. Ripmeester, *Chem. Commun.* **2000**, 1905–1906.
- [14] E. B. Brouwer, K. A. Udachin, G. D. Enright, J. A. Ripmeester, K. J. Ooms, P. A. Halchuk, *Chem. Commun.* **2001**, 565–566.
- [15] a) N. L. Allinger, Y. H. Yuh, J.-H. Lii, *J. Am. Chem. Soc.* **1989**, *111*, 8551–8566; b) J.-H. Lii, N. L. Allinger, *J. Am. Chem. Soc.* **1989**, *111*, 8566–8575; c) J.-H. Lii, N. L. Allinger, *J. Am. Chem. Soc.* **1989**, *111*, 8576–8582.
- [16] a) J. W. Ponder, F. Richards, *J. Comput. Chem.* **1987**, *8*, 1016–1024; b) C. Kundrot, J. W. Ponder, F. Richards, *J. Comput. Chem.* **1991**, *12*, 402–409; c) M. J. Dudek, J. W. Ponder, *J. Comput. Chem.* **1995**, *16*, 791–816.
- [17] a) T. Harada, J. M. Rudzinski, S. Shinkai, *J. Chem. Soc. Perkin Trans. 2* **1992**, 2109; b) T. Harada, J. M. Rudzinski, E. Osawa, S. Shinkai, *Tetrahedron* **1993**, *49*, 5941–5954; c) T. Harada, F. Ohseto, S. Shinkai, *Tetrahedron* **1994**, *50*, 13377–13394; d) V. Böhmer, R. Dörrenbächer, M. Frings, M. Heydenreich, D. de Paoli, W. Vogt, G. Ferguson, I. Thondorf, *J. Org. Chem.* **1996**, *61*, 549–559; e) S. Fischer, P. D. J. Grootenhuis, L. C. Groenen, W. P. van Hoorn, F. C. J. M. van Veggel, D. N. Reinhoudt, M. Karplus, *J. Am. Chem. Soc.* **1995**, *117*, 1611–1620.
- [18] S. Mecozi, J. Rebek, Jr., *Chem. Eur. J.* **1998**, *4*, 1016–1022.
- [19] R. Voorintholt, M. T. Koster, G. Vegter, G. Friend, W. G. J. Hol, *J. Mol. Graphics* **1989**, *7*, 243–245.
- [20] *Cerius²*, Molecular Simulation Software, Molecular Simulation Inc.
- [21] M. I. Ogden, A. L. Rohl, J. D. Gale, *Chem. Commun.* **2001**, 1626–1627.
- [22] For organic compounds, the Kitaigorodski index range is 0.65–0.77, see: a) A. I. Kitaigorodski, *Molecular Crystals and Molecules*, Academic Press, New York, **1973**, p. 167; b) G. R. Desiraju, *Crystal Engineering: The Design of Organic Solids*, Elsevier, New York, **1989**; c) A. Gavezzotti, *Acc. Chem. Res.* **1994**, *27*, 309–314. For proteins, the Kitaigorodski index range is 0.40–0.60, see: d) F. H. C. Crick, J. C. Kendrew, *J. Mol. Biol.* **1968**, *33*, 491–497; e) K. M. Andersson, S. Hormöller, *Acta Crystallogr.* **2000**, *D56*, 789–790.
- [23] a) G. D. Andreotti, R. Ungaro, A. Pochini, *J. Chem. Soc. Chem. Commun.* **1979**, 1005; b) R. Ungaro, A. Pochini, G. D. Andreotti, P. Domiano, *J. Chem. Soc. Perkin Trans. 2* **1985**, 197–201; c) G. D. Andreotti, O. Ori, F. Uguzzoli, C. Alfieri, A. Pochini, R. Ungaro, *J. Inclusion Phenom.* **1988**, *6*, 523–536; d) M. Takeshita, S. Nishio, S. Shinkai, *J. Org. Chem.* **1994**, *59*, 4032–4034; e) W. Xu, R. J. Puddephatt, K. W. Muir, A. A. Torabi, *Organometallics* **1994**, *13*, 3054–3062; f) B. Masci, *Tetrahedron* **1995**, *51*, 5459–5464; g) G. Wipff, M. Lauterbach, *Supramol. Chem.* **1995**, *6*, 187–207; h) K. N.

- Koh, K. Araki, A. Ikeda, H. Otsuka, S. Shinkai, *J. Am. Chem. Soc.* **1996**, *118*, 755–758; i) P. Lhotak, S. Shinkai, *J. Phys. Org. Chem.* **1997**, *10*, 273–285.
- [24] a) J. M. Rivera, T. Martin, J. Rebek, *J. Am. Chem. Soc.* **2001**, *123*, 5213–5220; b) A. Tanatani, M. J. Mio, J. S. Moore, *J. Am. Chem. Soc.* **2001**, *123*, 1792–1793; c) R. Warmuth, *Eur. J. Org. Chem.* **2001**, 423–437; d) F. Hof, C. Nuckolls, S. L. Craig, T. Martin, J. Rebek, Jr., *J. Am. Chem. Soc.* **2000**, *122*, 10991–10996; e) F. Hof, C. Nuckolls, J. Rebek, Jr., *J. Am. Chem. Soc.* **2000**, *122*, 4251–4252; f) M. O. Vysotsky, V. Bohmer, *Org. Lett.* **2000**, *2*, 3571–3574; g) Y. L. Cho, D. M. Rudkevich, J. Rebek, Jr., *J. Am. Chem. Soc.* **2000**, *122*, 9868–9869.

Received: January 10, 2002

Revised: June 18, 2002 [F3788]